Acta Geochim (2023) 42(1):1–8
https://doi.org/10.1007/s11631-022-00585-4

ORIGINAL ARTICLE

The discovery of TiO_2-II, the α-PbO_2-structured high-pressure polymorph of rutile, in the Suizhou L6 chondrite

Xiande Xie[1] · Xiangping Gu[2] · Ming Chen[1,3]

Received: 27 September 2022 / Revised: 23 October 2022 / Accepted: 3 November 2022 / Published online: 11 December 2022

Abstract We report the discovery of TiO_2-II in the unmelted rock of the shocked Suizhou L6 chondrite. Natural TiO_2-II was previously found in ultrahigh-pressure metamorphic and mantle-derived rocks, terrestrial impact structures, and tektite. Our microscopic, Raman spectroscopic, electron microprobe and transmission electron microscopic investigations have revealed: (1) All observed TiO_2-II grains are related with ilmenite and pyrophanite; (2) TiO_2-II occurs as needle- and leaf-shaped inclusions in ilmenite and patch-, tape-shaped body in pyrophanite; (3) The composition of TiO_2-II is identical with that of its precursor rutile; (4) The Raman spectrum of TiO_2-II is in good agreement with that of natural and synthesized α-PbO_2-type TiO_2; (5) TiO_2-II occurs mainly in the form of well-ordered nano-domains and small mis-orientation among the domains can be observed. (6) All electron diffraction reflections from TiO_2-II can be indexed to α-PbO_2 structure in space group *Pbcn* with lattice parameters of $a = 4.481$ Å, $b = 5.578$ Å and $c = 4.921$ Å; (7) The exsolution inclusions of rutile from host ilmenite are mostly connected with an alternation process along the lamellar twinning plane of ilmenite induced by shock-induced high pressure and high temperature; (8) The *P–T* regime of 20–25 GPa and 1000 °C estimated for the Suizhou unmelted rock is suitable for phase transition of rutile into TiO_2-II phase.

Keywords Rutile · TiO_2-II · High-pressure polymorph · Shock metamorphism · Suizhou meteorite

✉ Xiande Xie
xdxie@gzb.ac.cn

[1] Key Laboratory of Mineralogy and Metallogeny/Guangdong Provincial Laboratory of Mineral Physics and Materials, Guangzhou Institute of Geochemistry, Chinese Academy of Sciences, Guangzhou 510640, China

[2] School of Geosciences and Info-Physics, Central South University, Changsha 410083, China

[3] State Key Laboratory of Isotope Geochemistry, Guangzhou Institute of Geochemistry, Chinese Academy of Sciences, Guangzhou 510640, China

1 Introduction

Rutile is a common accessory mineral in various types of terrestrial and extraterrestrial rocks. TiO_2-II is a high-pressure polymorph of rutile that was first synthesized by static compression experiment (Bendeliany et al. 1966) and by shock wave techniques (McQueen et al. 1967). The powder X-ray diffraction data show that TiO_2-II is isostructural with α-PbO_2-type TiO_2, space group *Pbcn*, synthesized by shock experiments (McQueen et al. 1967) and in-situ high-pressure experiments using a diamond-anvil cell (Gerward and Olsen 1997). It was also revealed that TiO_2-II is the only high-pressure polymorph of rutile that can be recovered experimentally at ambient conditions (Wu et al. 2010).

The occurrence of natural TiO_2-II was previously reported in ultrahigh-pressure metamorphic rocks (Huang et al. 2000; Wu et al. 2005), mantle-derived rocks (Dobrzhinetskaya et al. 2009), terrestrial impact structures (El Goresy et al. 2001; Jackson et al. 2006; McHone et al. 2008; Chen et al. 2013), and tektite (Glass and Fries 2008), as well as in Neoarchean spherule layers (Smith et al. 2016), but no finding of TiO_2-II in meteorites was reported in the literature. In this paper, we report the discovery of

TiO_2-II in a meteorite, namely, in the shocked Suizhou L6 chondrite.

2 Samples and analytical methods

The Suizhou L6 chondrite fell on April 15, 1986, at Dayanpo, Suizhou City, Hubei Province, China. This meteorite consists of olivine, low-Ca pyroxene, plagioclase, FeNi-metal, troilite, merrillite, chlorapatite, chromite, ilmenite, pyrophanite, native copper, and shenzhuangite (Xie et al. 2001a, 2011; Xie and Chen 2016; Bindi and Xie 2017). Rutile is a very rare phase observed only inside some ilmenite and pyrophanite grains. The Suizhou meteorite was classified as a strongly shock-metamorphosed (S5) meteorite due to the presence of transformation of plagioclase to maskelynite (Xie et al. 2001a; 2011). This meteorite contains a few very thin shock-produced melt veins, and up to 14 high-pressure phases were identified inside or adjacent to these veins, among them, the ringwoodite, majorite, lingunite, magnesiowüstite and majorite-pyrope$_{s.s.}$ are abundant constituent high-pressure phases, but tuite, xieite, chenmingite, wangdaodeite, hemleyite, asimowite, poirierite, hiroseite and elgoresyite are new high-pressure minerals (Xie et al. 2001a, 2002, 2011, 2019; Chen et al. 2003, 2008; Ma et al. 2018; Xie and Chen 2016, Bindi et al. 2017, 2019, 2020, 2021; Tomioka et al. 2021).

Polished thin sections were prepared from fragments of the Suizhou meteorite. All observations and physical and chemical analyses are performed in-situ on thin sections. The mineral assemblages in polished sections of the samples were investigated by optical microscopy using a Leica DM2500p microscope. A Shimadzu 1720 electron microprobe (EPMA) was used to study the mineral occurrence in back-scattered electron (BSE) mode, and to quantitatively determine the chemical composition of minerals using the wave length dispersive technique at 15 kV accelerating voltage and beam current of 10 nA. Natural and synthetic phases of well-known compositions were used as standards, such as SiO_2 for Si, TiO_2 for Ti, Al_2O_3 for Al, Fe_3O_4 for Fe, and pure Mn, Nb, Ta, and the data were corrected using a ZAF program. Raman spectra of minerals in the polished thin sections were recorded with a Horiba Labram Aramis instrument. A microscope was used to focus the excitation beam (Ar+ laser, 633 nm line) to 1 μm wide spots and to collect the Raman signal. Accumulations of the signal lasted 300 s. The laser power was 2 mW. A focused ion (Ga+) beam (FIB) workstation equipped in the FEI Helios Nanolab 600i systems at the Center for Advanced Research of Central South University was used to cut a chip in sizes of 10 μm × 7 μm × 0.2 μm, which was mounted onto the molybdenum sample holder and then sliced to a thickness of about 37 nm for transmission electron microscopy (TEM) observation. TEM and selected area electron diffraction (SAED) analyses were performed using Fei Titan G2 60–300 transmission electron microscope operated at 300 kV accelerating voltage.

3 Results

3.1 Occurrence

Rutile occurs in the Suizhou chondritic rock as acicular and leaf-shaped crystals inside ilmenite grains (Fig. 1). However, rutile grains are seldom preserved without transformation to TiO_2-II in the un-melted chondritic part of the Suizhou meteorite. Most of them have transformed to their high-pressure polymorph—TiO_2-II. Under a reflected light microscope, both rutile and TiO_2-II can not be distinguished and shows a grayish color and brighter reflectance than coexisting ilmenite and pyrophanite in a specific polarized direction. Four types of occurrence of TiO_2-II, patch-shaped, tape-shaped, needle-shaped, and leaf-shaped grains are observed (Fig. 2): Fig. 2a shows two patch-shaped grains of 8 × 5 μm and 10 × 4 μm in sizes in grain with a transition composition between ilmenite and pyrophanite. For the upper-left and the lower-right TiO_2-II grains, some lamella-like slices of TiO_2-II can be observed. Besides, a long tape-shaped grain of 20 μm in length and 2 ~ 3 μm in width is also observed in this grain. Figure 2b shows some large patch-shaped TiO_2-II grains up to 30 × 12 μm in size, and a few tape-like grains of rutile. Figure 2c displays a needle-like TiO_2-II of 30 μm in length and 1–2 μm in width in a fractured ilmenite grain, and it crosses the whole ilmenite grain. Figure 2d shows two leaf-shaped TiO_2-II grains of 20 and 16 μm in length, and a

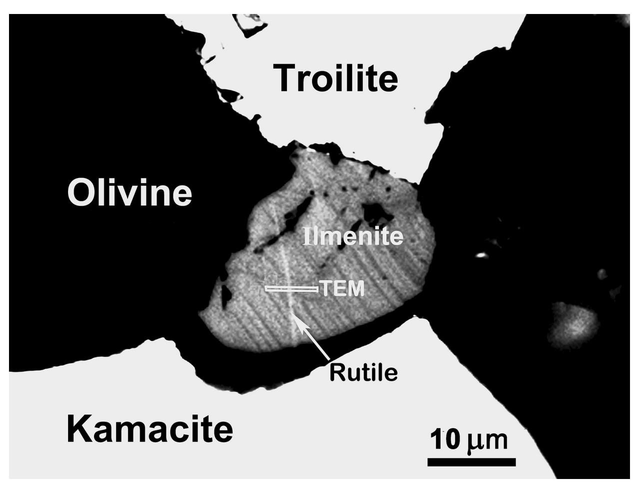

Fig. 1 Acicular crystal of rutile in ilmenite surrounded by kamacite, troilite, and olivine, the line with TEM indicates the position of the TEM chip

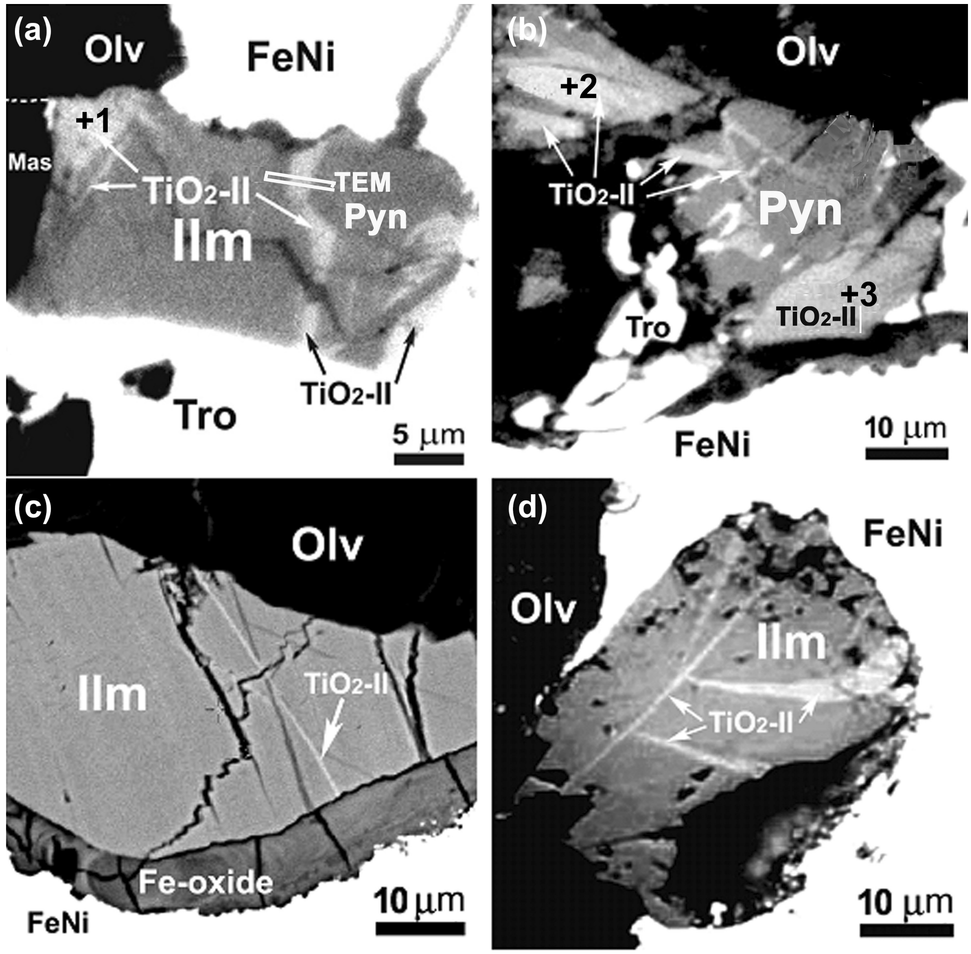

Fig. 2 Reflected light photomicrographs showing different occurrences of TiO_2-II in ilmenite (Ilm) and pyrophanite (Pyn) grains. **a** Patch-shaped TiO_2-II grains developed on both tops of pyrophanite and ilmenite grain and a tape-like TiO_2-II grain in the middle part of this grain. **b** Patch-shaped TiO_2-II grains in pyrophanite. **c** a TiO_2-II needle in an ilmenite grain. **d** Two leaf-shaped and needle-like TiO_2-II grains in ilmenite. Cr = chromite, Olv = olivine, Msk = maskelynite, FeNi = FeNi metal, Tro = troilite, Ru = rutile, Fe-oxide = amorphous Fe-oxide: The crosspoints with numbers 1, 2, and 3 refer to the positions of EPMA

needle-shaped TiO_2-II of 40 μm in length and 1.5–2 μm in width. Interestingly, all TiO_2-II-bearing ilmenite grains we observed in the Suizhou meteorite are surrounded by FeNi metal or FeNi metal + troilite and olivine.

3.2 Chemical composition

Quantitative analytical results of chemical compositions of TiO_2-II are given in Table 1. The compositions of TiO_2-II are similar to that of rutile that occurred in many meteorites (Ramdohr 1973) and Xiuyan impact crater (Chen et al. 2013). The TiO_2-II in Suizhou meteorite contains dominating TiO_2 with minor amounts of FeO (up to 2.06 wt%), MgO (up to 0.39 wt%), MnO (up to 0.97 wt%), Cr_2O_3 (up to 0.69 wt%) and Nb_2O_5 (up to 0.17 wt%). The empirical formula of TiO_2-II (based on total atoms = 3 *apfu*) can be written as $(Ti_{0.966}Fe_{0.023}Mn_{0.006}V_{0.006}Cr_{0.005}Mg_{0.004}Si_{0.001}Al_{0.001})_{1.013}O_{1.987}$. The simplified formula is TiO_2. This implies that TiO_2-II is formed from rutile by solid-state phase transformation under pressure.

3.3 Raman spectroscopy

Although the size of the TiO_2-II phase in the Suizhou meteorite is small and thin, and it closely coexists with ilmenite and pyrophanite, we could obtain good enough Raman spectra of TiO_2-II phase since this phase exhibits strong Raman scattering. Figure 3 shows the Raman

Table 1 Composition of TiO_2-II in the Suizhou meteorite

Sample[a]	TiO_2	SiO_2	Al_2O_3	Nb_2O_5	V_2O_3	Cr_2O_3	FeO	MgO	MnO	Total
1	92.97	0.04	0.10	0.00	0.54	0.55	3.71	0.39	0.97	99.33
2	99.41	0.06	0.08	0.17	0.61	0.21	0.94	0.00	0.21	101.68
3	95.81	0.08	0.08	0.06	0.56	0.69	1.52	0.19	0.44	99.42
Average	96.06	0.06	0.09	0.08	0.57	0.48	2.06	0.19	0.54	100.14

[a]Positions of sample numbers are shown in Fig. 2a, b

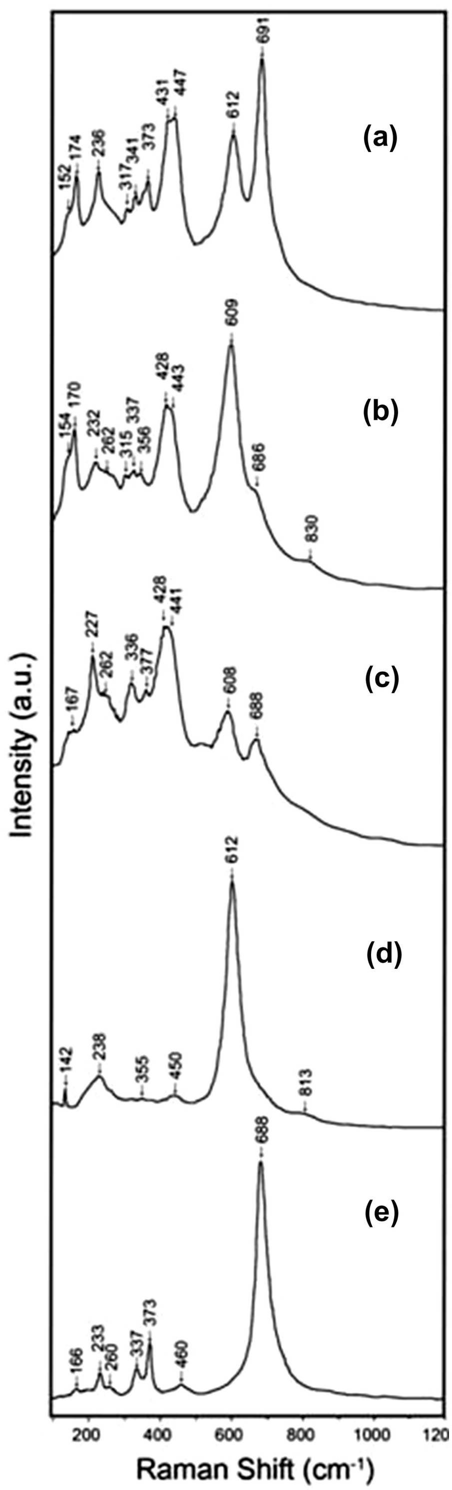

Fig. 3 Raman spectra of TiO_2 minerals in the Suizhou meteorite. **a** From a patch-shaped TiO_2-II on the up-right top of Fig. 2a with strong band of ilmenite (691 cm^{-1}) and that of rutile (612 cm^{-1}), **b** From a TiO_2-II needle shown in Fig. 2c. Note the 609 cm^{-1} band of rutile is very strong. **c** From a leaf-shaped TO_2-II grain shown in Fig. 2d with a minor amount of ilmenite and rutile. **d** Rutile coexisting with TiO_2-II, **e** Ilmenite coexisting with TiO_2-II

spectra of TiO_2-II, rutile, and ilmenite in the Suizhou meteorite. Raman spectra of TiO_2-II in Fig. 3a, b, c display well-defined peaks at 152–154 (m), 170–174 (s), 315–317 (w), 336–341 (m), 428–431 (vs), 441–447 (vs, sh), which are distinct from that of rutile at 142 (w), 238 (m, bd), 355 (w), 450 (w) and 612 (vs) cm^{-1} (Fig. 3d) (vs = very strong, s = strong; m = medium; w = weak; sh = shoulder, bd = broad). The spectrum of TiO_2-II is in good agreement with that of α-PbO_2-type TiO_2 found in shock-metamorphosed rutile in the Xiuyan impact crater (Chen et al. 2013) and that of TiO_2-II synthesized at static high pressures (Mammone et al. 1981). However, the presence of rutile peaks (608–612 cm^{-1}) on the Raman spectra of Suizhou TiO_2-II implies that some host rutile relict remained in TiO_2-II grains.

3.4 Crystallography

The crystal structure of TiO_2-II was determined by Filatov et al. (2007) using the single-crystal x-ray diffraction analysis, which is different from that of rutile. In both structures of TiO_2-II and rutile, chains of edge-sharing TiO_2 octahedra along the *c*-axis are connected through two vertices of each octahedron, forming the three-dimensional framework. An obvious difference in the structure between TiO_2-II and rutile lies in that the TiO_2-II structure consists of zigzag edge-sharing TiO_6 octahedral chains instead of straight edge-sharing octahedral chains as in rutile.

Since the grains of both rutile and TiO_2-II in the Suizhou meteorite are very thin and small, we could obtain their crystallographic data only by TEM observations. The results of our observations are described as follows.

3.4.1 TEM observations of rutile

A chip of needle-like rutile embedded in ilmenite prepared from focused ion beam (FIB) thinning is observed by TEM. Representative results are shown in Fig. 4. Figure 4a is the bright field image of needle-like rutile in ilmenite shown in Fig. 1, and Fig. 4b is the selected area electron diffraction (SAED) pattern of rutile along the zone-axis [100], which shows that all reflections are elongated indicating a deformed rutile structure. All reflections from rutile can be indexed to tetragonal structure in space group $P4_2/mnm$. Figure 4c is the high-resolution transmission electron microscopy (HRTEM) image of the needle-like rutile, in which the well-developed (hk0) stacking faults are observed. Figure 4d is the fast Fourier transform (FFT) pattern of rutile along the [010] zone-axis.

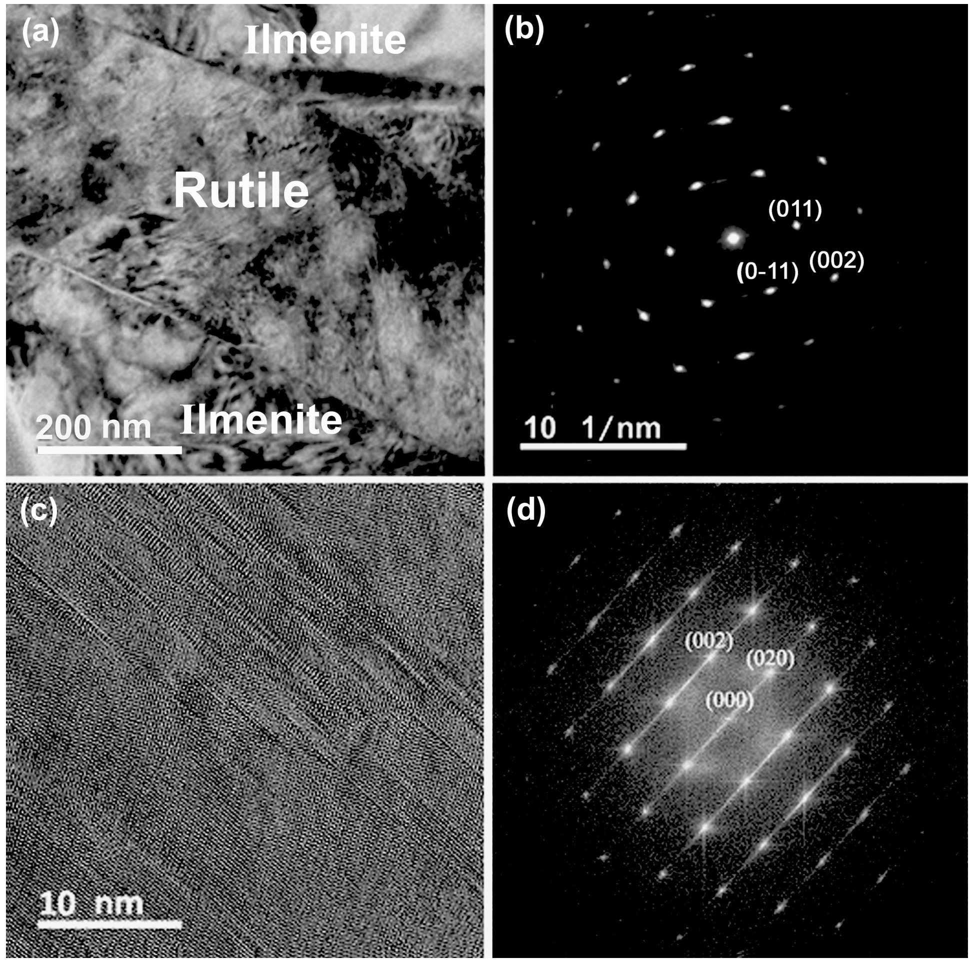

Fig. 4 TEM images of rutile in the Suizhou meteorite. **a** Bright field image of TiO_2 rutile needle in ilmenite. **b** SAED pattern of TiO_2 rutile along the zone-axis [100]. **c** HRTEM image of rutile. Note the well-developed (hk0) stacking faults. **d** Fast Fourier transform (FFT) pattern of rutile along [010] zone-axis

3.4.2 TEM observations of TiO_2-II

Chips of TiO_2-II phase embedded in pyrophanite prepared from focused ion beam (FIB) thinning are observed by TEM, Representative results are shown in Fig. 5. Figure 5a is the bright field image of the patch-shaped TiO_2-II grain shown in Fig. 2a, and the Fig. 5b is the SAED pattern of TiO_2-II along [010] zone-axis. All reflections from TiO_2-II can be indexed to α-PbO_2 structure in space group *Pbcn* with lattice parameters of a = 4.581 Å, b = 5.578 Å, c = 4.921 Å, V = 125.74 Å^3, Z = 4. The spots pointed by arrows may be from diffuse reciprocal rods of the first-ordered Laue zone. Figure 5c, d are HRTEM images and FFT patterns of patch-shaped TiO_2-II along the [010] zone-axis, respectively. On the HRTEM image nano-domains with *Pbcn* symmetry are clearly shown, and small mis-orientation among the domains can be detected. FTT image from some TiO_2-II domains looks well-ordered and do not show extra spots that violate the c-glide. However, in some boundary/interface areas it shows spots that violate the c-glide.

The structure data obtained for TiO_2-II in the Suizhou meteorite using the electron diffraction method are consistent with those obtained for the shock-induced TiO_2-II in the Xiuyan impact crater using micro X-ray diffraction analyses, which showed an α-PbO_2-type *Pbcn* structure and lattice parameters of a = 4.543(1)Å, b = 5.491(9)Å, c = 4.895(2)Å, V = 122.1(4) Å^3, Z = 4. (Chen et al. 2013). The slight difference in cell parameters between TiO_2-II in the Suizhou chondrite and Xiuyan impact crater can be explained by the difference in the precision of measurement.

4 Discussion and conclusion

Ramdohr (1973) reported that almost all ilmenite grains in meteorites show marked lamellar twinning caused by pressure, and they sometimes contain exsolution inclusions of another mineral, probably caused by twin lamellation, He mentioned that rutile in many normal chondrites is often associated with ilmenite and chromite, sometimes intimately intergrown, frequently as large individual

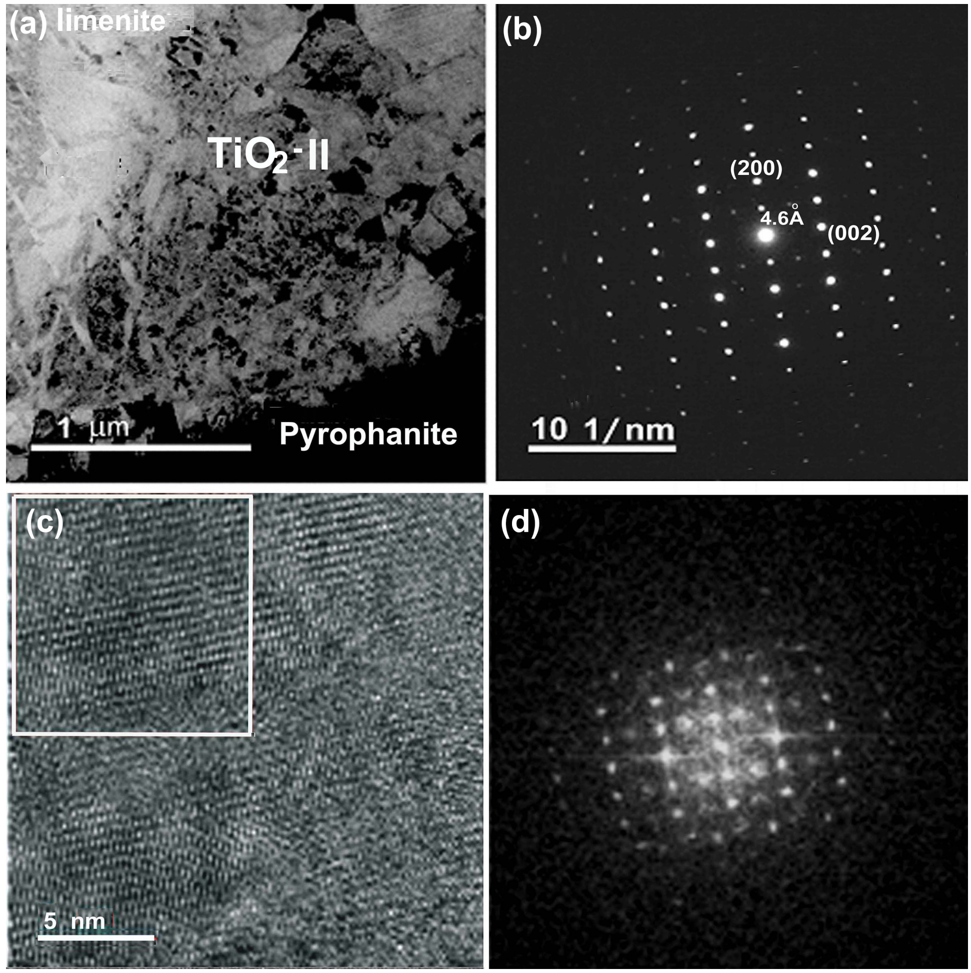

Fig. 5 TEM images of patch-shaped TiO_2-II in the Suizhou meteorite. **a** Bright field image of patch-shaped TiO_2-II with α-PbO_2-type *Pbcn* structure. **b** SAED pattern of TiO_2-II along [010] zone-axis, **c** HRTEM image of TiO_2-II. Note the square area on its up-left is for FFT analysis **d** FFT pattern of TiO_2-II along [010] zone-axis

grains. The inclusion of rutile in ilmenite is mostly connected with an alternation process, but very thin lamellae of rutile can be present in ilmenite without recognizable signs of an alternation. He also reported that ilmenite grains in many chondrites contain a few straight and very thin lamellae of rutile, often only one, crossing the whole ilmenite grain.

Ilmenite, $FeTiO_3$, is one of the accessory opaque minerals in the Suizhou L6 chondrite. It occurs in association with troilite, chromite, and FeNi metal as small grains of irregular shape with grain sizes less than 20–30 μm. The ilmenite content in this meteorite is only about 20 ppm by volume. Our TEM study revealed that ilmenite in the Suizhou meteorite also shows marked lamellar twinning caused by shock-induced pressure, and a straight fracture in parallel with the lamellar twinning is visible. Rutile in the Suizhou chondrite is associated with ilmenite as inclusions and most rutile grains have transformed to TiO_2-II. Based on the occurrences of TiO_2-II and its close relations with ilmenite, we assume that all four types of TiO_2-II occurrence are consistent with that of rutile in many other chondrites described by Ramdohr (1973).

The replacement structure of ilmenite in Suizhou can be seen in Fig. 2a, where the two patch-shaped TiO_2-II grains show lamellar structure. This implies that the replacement process would have started at the tiny exsolution lamellae of precursor rutile. The occurrence and the form of the replacement of ilmenite by precursor rutile would presume the reaction proposed by Ramdohr (1973): $2\ FeTiO_3 + C$ (as a hydrocarbon) $= 2\ Fe + 2\ TiO_2 + CO_2$. A similar alternation mechanism can be explained for the formation of leaf-shaped TiO_2 -II grains shown in Fig. 2d. As for the thin and straight needle-like TiO_2-II shown in Fig. 2c and the tape-like TiO_2-II shown in Fig. 2a, no signs of alternation were observed. This can be explained by the exsolution of TiO_2 along one of the rhombohedron faces (Ramdohr 1973) or in parallel with the lamellar twinning plane of ilmenite caused by shock-induced pressure and temperature.

After Bendeliany et al. (1966) first synthesized TiO_2-II by static compression experiment, several high-pressure experiments revealed that rutile can be transformed not only into a high-pressure polymorph of TiO_2-II (α-PbO_2), but also into baddeleyite, orthorhombic I and cotunnite phases with increasing pressure (Nishio-Hamane et al. 2010, and references therein), and the high-pressure polymorphs of baddeleyite, orthorhombic-I, and cotunnite-type TiO_2 would reverse to TiO_2-II on decompression. Several static compression experiments succeed in the transition of rutile to TiO_2-II at a pressure range between 4 and 12 GPa and temperature between 400 and 1500 °C (Bendeliany et al. 1966; Jamieson and Olinger 1968; Akaogi et al. 1992; Olsen et al. 1999; Withers et al. 2003). Shock-loading experiments revealed that rutile transforms to TiO_2-II at peak shock pressure from 20 to 100 GPa (McQueen et al. 1967; Linde and Decarli 1969; Kusaba et al. 1988). Based on shock compression experiments, Kusaba et al. (1988) proposed a displacive mechanism of phase transition to explain the shock-produced transformation of rutile to TiO_2-II, in which rutile first transforms by shock compression to a high-pressure polymorph, and then this polymorph instantly converts to TiO_2-II structure during decompression. Based on the static and shock compression experiments, it is reasonable to assume that the transition of rutile to TiO_2-II takes place at static high pressure of 4–12 GPa and high temperature of 400–1500 °C, and peak shock pressure from 20 to 100 GPa.

Wu et al. (2010) reported that TiO_2-II is the only high-pressure polymorph that can be recovered experimentally at ambient conditions. Therefore, the presence of natural TiO_2-II in ultrahigh-pressure metamorphic rocks, mantle-derived rocks, terrestrial impact structures, and tektite is quite understandable.

The Suizhou meteorite is a heavily shocked chondrite. Most of the plagioclase grains in Suizhou unmelted chondritic rock display isotropic nature indicating these grains have transformed into maskelynite, a melted plagioclase glass. This indicates that the Suizhou unmelted rock experienced a peak shock pressure of 20–25 GPa and a temperature of 1000 °C (Xie et al. 2001b, 2011; Xie and Chen 2016). This shock-induced *P–T* regime in the Suizhou unmelted chondritic rock is suitable for the phase transition of rutile into the TiO_2-II phase because it falls in the *P–T* range of such phase transition determined by both static and shock-loading experiments.

Acknowledgements The authors are grateful to Professor Huifang Xu of the Department of Geoscience, University of Wisconsin-Madison, U.S.A, for his help in dealing with the TEM images of TiO_2-II phase.

Declarations

Conflict of interest The authors declare that they have no conflict of interest.

References

Akaogi M, Kusaba K, Susaki J, Yagi T, Matsui M, Kikegawa T, Yusa H, Ito E (1992) High-pressure high-temperature stability of α-PbO_2-type TiO_2 and $MgSiO_3$ majorite: calorimetric and in situ X-ray diffraction studies. In: Syono Y, Manghnani MH (eds) High-pressure research: application to Earth and planetary sciences, vol 67. Terra Scientific/American Geophysical Union, Tokyo/Washington DC, pp 447–455

Bendeliany NA, Popova SV, Vereschagin LF (1966) New modification of titanium dioxide obtained at high pressures. Geokhimiya 5:499–502

Bindi L, Xie XD (2017) Shenzhuangite, a new mineral. Eur J Miner 29:779

Bindi L, Chen M, Xie XD (2017) Discovery of the Fe-analogue of akimotoite in the shocked Suizhou L6 chondrite. Sci Rep 7:42674

Bindi L, Brenker FE, Nestola F, Koch TE, Prior DJ, Lilly K, Krot AN, Bizzarro M, Xie XD (2019) Discovery of asimowte, the Fe-analog of wadsleyite, in shock-melted silicate droplets of the Suizhou L6 and the Quebrada Chimborazo 001 CB3.0 chondrites. Am Miner 104:775–778

Bindi L, Shim SH, Sharp TG, Xie XD (2020) Evidence for the charge disproportionation of iron in extraterrestrial bridgmanite. Sci Adv 6(2):6

Bindi L, Sinmyo R, Bykova E, Ovsyannikov SV, McCammon C, Ilya Kupenko I, Ismailova L, Dubrovinsky L, Xie XD (2021) Discovery of elgoresyite, $(Mg, Fe)_5Si_2O_9$: implications for novel iron-magnesium silicates in rocky planetary interiors. ACS Earth Sp Chem 5:2024–2130

Chen M, Shu JF, Xie XD, Mao HK (2003) Natural $CaTi_2O_4$-structured $FeCr_2O_4$ polymorph in the Suizhou meteorite and its significance in mantle mineralogy. Geochim Cosmochim Acta 67(20):3937–3942

Chen M, Shu JF, Mao HK (2008) Xieite, a new mineral of high-pressure $FeCr_2O_4$ polymorph. Chin Sci Bull 53(21):3341–3346

Chen M, Gu XP, Xie XD, Yin F (2013) High-pressure polymorph of TiO_2-II from the Xiuyan crater of China. Chin Sci Bull 58:4655–4662

Dobrzhinetskaya LF, Wirth R, Yang J, Hutcheon ID, Weber PK, Green HW II (2009) High-pressure highly reduced nitrides and oxides from chromitite of a Tibetan ophiolite. Proc Natl Acad Sci USA 106:19233–19238

Filatov SK, Bendeliani NA, Albert B, Kopf J, Dyuzheva TI, Lityagina LM (2007) Crystalline structure of the TiO_2 II high-pressure phase at 293, 223, and 133K according to single-crystal x-ray diffraction data. Dokl Phys 52:195–199

El Goresy A, Chen M, Gillet P, Dubrovinsky L, Graup G, Ahuja R (2001) A natural shock-induced dense polymorph of rutile with α-PbO_2 structure in the suevite from the Ries crater in Germany. Earth Planet Sci Lett 192:485–495

Gerward L, Olsen JS (1997) Post-rutile high-pressure phase in TiO_2. J Appl Crystallogr 30:259–264

Glass B, Fries M (2008) Micro-Raman spectroscopic study of fine-grained, shock-metamorphosed rock fragments from the Australasian microtektite layer. Meteorit Planet Sci 43:1487–1496

Huang SL, Shen P, Chu HT, Yui TF (2000) Nanometer-size α-PbO_2-type TiO_2 in garnet: a thermobarometer for ultrahigh-pressure metamorphism. Science 288:321–324

Jackson JC, Horton JW, Chou IM, Belkin HE (2006) A shock-induced polymorph of anatase and rutile from the Chesapeake Bay impact structure, Virginia, USA. Am Miner 91:604–608

Jamieson J, Olinger B (1968) High-pressure polymorphism of titanium dioxide. Science 161:893–895

Kusaba K, Kikuchi M, Fukuoka K, Syono Y (1988) Anisotropic phase transition of rutile under shock compression. Phys Chem Miner 15:238–245

Linde R, Decarli PS (1969) Polymorphic behavior of titania under dynamic loading. J Chem Phys 50:319–325

Ma C, Tschauner O, Beckett JR, Liu Y (2018) Discovery of chenmingite, $FeCr_2O_4$, with orthorhombic $CaFe_2O_4$-type structure, a shock-induced high-pressure mineral in the Tissint Martian meteorite. Lunar Planet Sci Conference 49:2083

Mammone JF, Nicol M, Sharma SK (1981) Raman spectra of TiO_2-II, TiO_2-III, SnO_2 and GeO_2 at high pressure. J Phys Chem Solids 42:379–384

McHone JF, Fries MD, Killgore M (2008) Raman detection of titania-II, an impact induced rutile polymorph in suevite ejecta at Bosumptwi crater. Ghana Lunar Planet Sci Conf 39:2450

McQueen RG, Jamieson JC, Marsh SP (1967) Shock-wave compression and X-ray studies of titanium dioxide. Science 155:1401–1404

Nishio-Hamane D, Shimizu A, Nakahira R, Niwa K, Sano-Furukawa A, Okada T, Yagi T, Kikegawa T (2010) The stability and equation of state for the cotunnite phase of TiO_2 up to 70 GPa. Phys Chem Miner 37:129–136

Olsen JS, Gerward L, Jiang JZ (1999) On the rutile/α–PbO_2-type phase boundary of TiO_2. J Phys Chem Solids 60:229–233

Ramdohr P (1973) The opaque minerals in stony meteorites. Elsevier Publishing Company, Amsterdam-London-New York, pp 48–54

Smith FC, Glass BP, Simonson BM, Smith JP, Knull-Davatzes AE (2016) Shock-metamorphosed rutile grains containing the high-pressure polymorph TiO_2-II in four Neoarchean spherule layers. Geol Soc Am 44(9):775–778

Tomioka N, Bindi L, Okuchi T, Miyahara M, Iitaka T, Li Z, Kawatsu T, Xie XD, Purevjav N, Tani R, Kodama Y (2021) Poirierite, a dense metastable polymorph magnesium iron silicate in shocked meteorites. Nat Commun Earth Environ 2:16. https://doi.org/10.1038/s43247-020-00090-7

Withers AC, Essene EJ, Zhang Y (2003) Rutile/TiO_2 II phase equilibria. Contrib Miner Petrol 145:199–204

Wu X, Meng D, Han Y (2005) α-PbO_2-type nanophase of TiO_2 from coesite-bearing eclogite in the Dabie Mountains, China. Am Miner 90:1458–1461

Wu X, Holbig E, Steinle-Neumann G (2010) Structural stability of TiO_2 at high pressure in density-functional theory based calculations. J Phys Condens Matter 22:295501

Xie XD, Chen M (2016) Suizhou meteorite: mineralogy and shock metamorphism. Springer-Verlag Heidelberg Berlin and Guangdong Science and Technology Press Co. Ltd., p 256

Xie XD, Chen M, Wang DQ (2001a) Shock-related mineralogical features and P-T history of the Suizhou L6 chondrite. Eur J Miner 13:1177–1190

Xie XD, Chen M, Dai CD, El Goresy A, Gillet P (2001b) A comparative study of naturally and experimentally shocked chondrites. Earth Planet Sci Lett 187:345–356

Xie XD, Minitti ME, Chen M, Wang DQ, Mao HK, Shu JF, Fei YW (2002) Natural high-pressure polymorph of merrillite in the shock vein of the Suizhou meteorite. Geochim Cosmochim Acta 66:2439–2444

Xie XD, Sun ZY, Chen M (2011) The distinct morphological and petrological features of shock melt veins in the Suizhou L6 chondrite. Meteorit Planet Sci 46:459–469

Xie XD, Gu XP, Yang HX, Chen M (2019) Wangdaodeite, the $LiNbO_3$-structured high-pressure polymorph of ilmenite, a new mineral from the Suizhou L6 chondrite. Meteorit Planet Sci 55:184–192